Journal of Chromatography, 282 (1983) 3–26
Elsevier Science Publishers B.V., Amsterdam — Printed in The Netherlands

CHROMSYMP. 124

THE ROLE OF BONDED PHASE COMPOSITION ON THE LIGAND-EXCHANGE CHROMATOGRAPHY OF DANSYL-D,L-AMINO ACIDS

B. FEIBUSH, M. J. COHEN and B. L. KARGER*
Institute of Chemical Analysis and Department of Chemistry, Northeastern University, Boston, MA 02115 (U.S.A.)

SUMMARY

This paper examines the role of bonded phase composition in the ligand-exchange chromatographic separation of dansyl amino acids (Dns-D,L-AAs). As the bonded optically active chelate, we have synthesized N-ω-(dimethylsiloxyl)undecanoyl-L-valine and as the metal, we used Cu(II). Bonded phases, where the chelate coverage is 2.5 μmol/m^2, have been compared with mixed or diluted phases, in which the contribution of the bonded chelate to the total coverage is less than 0.2 μmol/m^2. Using a decyl group as diluent, it has been shown that capacity factors and enantioselectivities of Dns-D,L-AAs are much higher on the diluted phases relative to the concentrated phase, in spite of the fact that the amount of copper loaded on the latter column is roughly 40 times greater. This result has been interpreted in terms of the formation of bis complexes between the metal ion and the bonded phase chelate, *i.e.*, 2:1 chelate to metal, in the case of the concentrated phase. For the diluted phases, the mono complex, *i.e.*, 1:1 metal to chelate, is the predominant form. Not only does the diluted phase yield improved separation, but it is in principle a simpler system to manipulate and optimize. We have been able to develop a simple model to analyze the chromatographic behavior on diluted phases relative to the concentrated phase. Based on this model, we have compared four diluents: a polyether, *n*-butyl, *n*-decyl and *n*-eicosyl ligands. By normalizing for the amount of copper loaded on the stationary phase, it is shown that the apparent complexation constants increase from the ether to the C_{20} phase. Moreover, due to differences in the character of the side chains of the amino acids, additional selectivity is observed between the different solutes. This selectivity is useful in separation applications. In addition, it is shown that the diluted bonded phases yield high performance, approximately 4000 plates for 15 cm columns, with good peak symmetry. Also included is a detailed discussion of the characterization of the bonded phases along with its optical purity.

INTRODUCTION

Ligand-exchange chromatography (LEC) is being actively pursued by several laboratories for the separation of enantiomers[1,2]. In general, two approaches to on-line chiral resolution by high-performance liquid chromatography (HPLC) have been

0021-9673/83/$03.00

advanced. The first approach involves the use of a chiral resolving agent, or additive, in the mobile phase[3]. The additive approach has been shown to be a practical solution to enantiomeric separation[4–11]. It is possible by this method to obtain high enantioselectivity and efficiency. In addition, the resolving agent is easily removed from the column, allowing for a non-dedicated system which can then be regenerated when needed.

The second approach employs a chiral, chemically bonded stationary phase. Relative to the additive approach, bonded phases encompass a broader potential range of operating conditions. The partitioning of the chiral additive is influenced by such factors as the mobile phase composition, pH, temperature, etc. In addition, the resolving agent and the conditions of its use are limited to those which do not generate a significant detector response. Bonded phases would also tend to be more usable in preparative-scale operation.

A substantial amount of research has been performed on the use of chiral agents bonded to polymeric supports. Amino acids[12–14] and N′,N′-dibenzyl-1,2-propanediamine[15], for example, have been bonded to polystyrene and polyacrylamide, and, using Cu(II) or Ni(II) as the complexing metal, α-amino acid enantiomers have been resolved with high enantioselectivity. However, these types of supports are generally limited in efficiency.

Recently, chiral compounds have been bonded to silica gel for use in ligand-exchange enantiomeric separation[16–21]. The utilization of small particle diameter silica gels, as support, results in high performance conditions in the normal- and reversed-phase modes. In the case of bonded ligand exchangers, high enantioselectivity is observed, but the chromatographic peaks are often characterized by low efficiency and asymmetry.

The use of a chiral additive results in an efficient ligand-exchange system, as a consequence of the relatively rapid equilibria between the various coordinated species. When a chelate is fixed to the silica surface, the exchange process might be restricted or even eliminated, depending on the accessibility of the active site. With different environments around and compositions of the active sites, a series of complexes may be generated having varying activities towards the solute. This heterogeneity of complexation may be a cause of broad and asymmetrical peaks. In addition, the distribution between these different species will directly affect retention and separation.

The goal of this work was to produce bonded ligand-exchange stationary phases where identical active sites are operating within a similar environment. This goal can be approached by: (a) removing the active site from the influence of the polar surface; (b) isolating each active site from interaction with other sites; and (c) ensuring the homogeneity of the medium surrounding the active site. N-ω-(Dimethylsiloxyl) undecanoyl-L-valinato copper(II) was used as the active chelate in this study.

In order to minimize the effect of the surface, in (a) above, we chose the available undecanoyl leash. As in affinity chromatography[22], a long spacer also increases the accessibility of the solute to the active site.

In an attempt to isolate the active sites (b), we explored the approach of diluted phases. By co-bonding the active chelate with a diluent, we adjusted the chelate surface concentration to be low enough to allow predominantly a 1:1 chelate:metal complex. Moreover, a monofunctional silane was used for bonding in order to preclude the possibility of partial prepolymerization, resulting in isolated patches of chelate.

The homogeneity of the medium surrounding the active site (c) is ensured by using a diluent. In this study, we have examined the effect of the type of diluent on the active site. By selecting an *n*-butyl or polyether diluent, we can envision surrounding the site with a medium similar to the mobile phase; by choosing an *n*-eicosyl diluent, the site is covered by a more hydrophobic environment; when an *n*-decyl diluent is used, the site is located at the mobile phase–stationary phase interface.

Since this work deals with subtle changes in the composition of the bonded surface, it has been necessary to develop sensitive analytical methods of characterization. These methods are also detailed in this work.

EXPERIMENTAL

Equipment

Two liquid chromatographs were assembled from components of various manufacturers. One system consisted of a Model M6000A pump and a Model 440 UV absorbance detector (λ = 254 nm) (Waters Assoc., Milford, MA, U.S.A.), a Model 7010 injection valve and a Model 7000 six-port rotary valve (Rheodyne, Cotati, CA, U.S.A.) and a Model 7127A strip-chart recorder and a Model 3390A reporting integrator (Hewlett-Packard, Palo Alto, CA, U.S.A.). The second system consisted of a Model 100 pump (Beckman Instruments, Berkeley, CA, U.S.A.), a Model 7120 injection valve (Rheodyne) and a Model FS970 fluorometer (excitation, 250 nm; emission 470 nm) (Kratos Analytical Instruments, Ramsey, NJ, U.S.A.) and a Model 156 strip-chart recorder (Linear Instruments, Reno, NV, U.S.A.). Both systems also included column-temperature controls —a Model NBE water-bath (Haake Buchler Instruments, Saddle Brook, NJ, U.S.A.) or a column heater (Jones Chromatography, Columbus, OH, U.S.A.). Gas chromatographic (GC) analyses were conducted with a Model 5730A gas chromatograph (Hewlett-Packard). Proton NMR spectra were taken on a Model T-60 NMR (Varian Assoc., Palo Alto, CA, U.S.A.).

Chemicals and supplies

Reagent grade L-valine, L-valine methyl ester hydrochloride, 10-undecenoic acid, 1-decene, trifluoroacetic acid, hexachloroplatinic acid, allyl bromide, diethylene glycol monomethyl ether and N-methylmorpholine were obtained from Aldrich (Milwaukee, WI, U.S.A.). All inorganic reagents, acetonitrile (HPLC grade) and reagent grade disodium ethylenediaminetetraacetate (EDTA) were obtained from J. T. Baker (Phillipsburgh, NJ, U.S.A.). HPLC grade *p*-dioxane was purchased from Burdick & Jackson Labs. (Muskegon, MI, U.S.A.). Distilled water was produced by a Model AG-11 still (Corning Glass Works, Corning, NY, U.S.A.). Reagent grade cupric acetate monohydrate was obtained from Mallinckrodt (St. Louis, MO, U.S.A.). Isobutylene was purchased from Matheson (Gloucester, MA, U.S.A.). Dimethylchlorosilane, *n*-butyldimethylchlorosilane, *n*-decyldimethylchlorosilane and hexamethyldisilazane were purchased from Petrarch Systems (Bristol, PA, U.S.A.). All optically active and racemic, free and dansylated amino acids, dansyl chloride, 1-eicosene and isobutyl chloroformate were obtained from Sigma (St. Louis, MO, U.S.A.). The IRA-400 strongly basic anion-exchange resin was purchased from Rohm & Haas (Philadelphia, PA, U.S.A.). In addition, silica gel (5 μm, nominal pore

size 100 Å, surface area 159 m^2/g, measured by manufacturer), column hardware and Porapak Q were obtained from Supelco (Bellefonte, PA, U.S.A.).

Synthesis

The synthetic strategy is shown in Fig. 1. The protected optically active amino acid *tert.*-butyl ester was first added to 10-undecenoic acid, followed by hydrosilylation and bonding to silica. Separate studies revealed that it was necessary to block the carboxylic acid group of L-valine (see 1) prior to the hydrosilylation reaction. Hydrosilylation of N-ω-undecenoyl-L-valine yielded a partially racemized product. Furthermore, endcapping was also conducted before deblocking of the carboxylic acid in order to avoid the otherwise observed racemization (see step 4 in Fig. 1).

L-Valine tert.-butyl ester. The method of Roeske[23] was used to prepare the *tert*-butyl ester of L-valine from the amino acid and isobutylene. The ester was precipitated from diethyl ether as the oxalate by the dropwise addition of a solution of 10% oxalic acid in absolute ethanol. After it was filtered and washed with diethyl ether, the salt was dried overnight in a vacuum dessicator. Yield 30%; m.p. 160–161°C.

The salt was then added to 1 *M* NaOH and extracted with diethyl ether. The organic layer was washed with water, dried over sodium sulfate and the solvent was removed. Yield 90%; colorless liquid. Thin-layer chromatography (TLC) on silica gel with 2% acetic acid in ethanol showed only one spot, $R_F = 0.63$, with ninhydrin spray detection. Optical purity ≥99.9%.

N-ω-Undecenoyl-L-valine tert.-butyl ester (I). Compound I was prepared by the mixed anhydride procedure, as described by Anderson *et al.*[24], using tetrahydrofuran (THF) as the solvent, N-methylmorpholine as the base and isobutyl chloroformate. After extraction with tartaric acid, the crude material was eluted through a bed of freshly regenerated IRA-400 OH anion-exchange resin by using methanol as the solvent, in order to remove unreacted 10-undecenoic acid. This material was

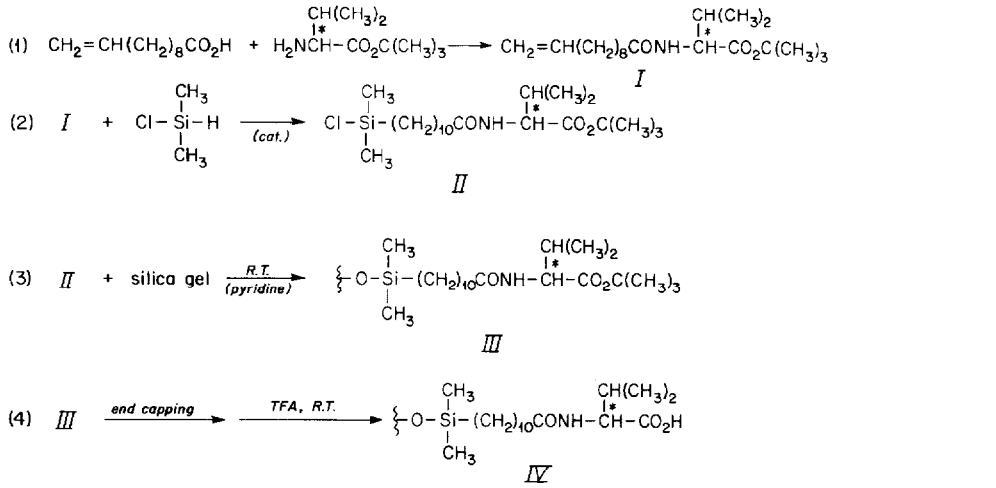

Fig. 1. Synthetic scheme of chiral-bonded chelate.

further purified by column chromatography on silica gel 60 with toluene, followed by 5% ethyl acetate as the eluent. TLC on silica gel showed one spot. Yield 85%; oily material. Elemental analysis: calculated C 70.75%, H 10.98%, N 4.13%; found C 70.83%, H 11.13%, N 4.28%. ^{1}H NMR: δ 0.90, 0.93 (2d, J 6.5 Hz, $2CH_3$), 1.29 [m, $W_{1/2}$ 5 Hz, $(CH_2)_6$], 1.46 [s, $(CH_3)_3C$], 1.7–2.4 (m, CH isopropyl, CH_2 allyl, CH_2CO), 4.44 (dd, J 8.5 and 4.5 Hz, $NCHCO_2$), 4.6–5.1 (m, CH_2 vinyl), 5.4–6.1 (m, CH vinyl), 6.33 (d, J 8.5 Hz, NH).

N-ω-Undecenoyl-L-valine methyl ester. The methyl ester analog of I was prepared in an identical manner by using L-valine methyl ester. Yield 80%; oily material. ^{1}H NMR as for I except δ 3.68 (s, CO_2CH_3) instead of δ 1.46.

N-ω-(Chlorodimethylsilyl)undecanoyl-L-valine tert.-butyl ester (II). An adaptation of the hydrosilylation reaction described by Speier *et al.*[25] was used. A 11-mmol sample of I was dissolved in 5.0 ml (ethanol-free) chloroform. To this solution, 45 mmol dimethylchlorosilane were added. Reflux was started, and a small amount of hexachloroplatinic acid added. Reflux was maintained for 1 h; then the volatiles were removed under <0.2 Torr at room temperature. Oily material. ^{1}H NMR: δ 0.42 [s, $Si(CH_3)_2$], 0.90, 0.93 (2d, J 6.5 Hz, $2CH_3$), 0.8–1.1 (m, $SiCH_2$), 1.29 [m, $W_{1/2}$ 6 Hz, $(CH_2)_8$], 1.46 [s, $(CH_3)_3C$], 1.95–2.5 (m, CH isopropyl, CH_2CO), 4.44 (dd, J 8.5 and 4.5 Hz, $NCHCO_2$), 6.43 (d, J 8.5 Hz, NH).

1-Allyloxy-2-(2'-methoxyethoxy)ethane. The sodium salt of diethylene glycol monomethyl ether, in dry toluene, was allowed to react with an equivalent amount of allyl bromide by the Williamson method. The product was purified by chromatography on silica gel, followed by fractional distillation. Yield 62%; colorless liquid, b.p. 49°C at 1.5 Torr. ^{1}H NMR: δ 3.30 (s, OCH_3), 3.64 [m, $W_{1/2}$ 4 Hz, $(CH_2CH_2O)_2$], 4.04 (d, J 5.5 Hz, CH_2 allyloxy), 5.0–5.5 (m, CH_2 vinyl), 5.6–6.3 (m, CH vinyl).

Mixed monochlorosilanes. Mixed silanes, needed to generate the diluted phases, were synthesized by co-hydrosilylation of a chloroform solution of the two appropriate olefins in the desired mole ratio by the procedure used for II. This method was used for all olefins, except volatile 1-butene. In that case, *n*-butyldimethylchlorosilane was mixed with II in the desired proportion.

Bonding of phases

A sample of 10 mmol of the appropriate monochlorosilane(s) was dissolved in 20 ml of dry pyridine. This solution was filtered directly through a 0.45-μm fluorocarbon filter onto 3.0 g of dried silica. The mixture was slowly rotated at room temperature for at least 5 h. The silica was then filtered and thoroughly washed with dichloromethane and methanol. The silica was dried at 60°C and endcapped with hexamethyldisilazane in pyridine, followed by filtering and washing as above.

Removal of tert.-butyl ester protective group. The above bonded phases were added to 25 ml of trifluoroacetic acid and rotated gently for 2 h. Subsequently, the silica was filtered and thoroughly washed with 10% water in methanol, followed by methanol, and then dried at 60°C.

Packing of columns

The packing of the various phases into 15 cm × 4.6 mm I.D. stainless-steel columns followed standard slurry producedures using a solution of methanol in car-

bon tetrachloride as slurry medium and a Model DSTV 122 air-driven pump (Haskel, Burbank, CA, U.S.A.).

Characterization of phases

Elemental analysis was performed by Galbraith Labs. (Knoxville, TN, U.S.A.). Determination of optical purity and ligand coverage was performed by hydrolysis of the amide linkage, dansylation of the generated D- and L-valine and injection into the liquid chromatograph that contained an appropriate chiral column. A sample of silica gel, typically 100 mg, was hydrolysed in 20 ml of boiling 75% aqueous (w/w) trifluoroacetic acid (TFA), containing a small amount of D-leucine as an internal standard. After a short time, ≈ 1 ml was removed for the determination of optical purity (see later discussion). The remainder of the sample was refluxed for 5 h and analyzed for total valine content per gram bonded material.

Each of the samples was stripped of the volatiles at high vacuum and dansylated by the procedure of Tapuhi *et al.*[26]. Injection of the dansylated sample into an LC ligand-exchange chiral column gave baseline resolution of the solutes. A typical chromatogram is shown in Fig. 2.

Optical purity (OP) was determined from the initially removed hydrolysate sample by the following equation:

$$\%\mathrm{OP} = 100 \times \left[\frac{\text{Area (L)} - \text{Area (D)}}{\text{Area (L)} + \text{Area (D)}}\right] \quad (1)$$

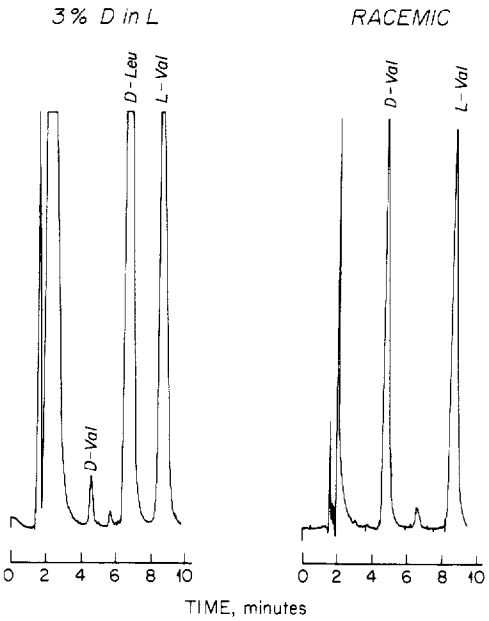

Fig. 2. Dns-D,L-Val analysis for optical purity and coverage. C_{10} diluted phase, 10^{-4} *M* Cu(II), 30% acetonitrile, 0.11 *M* acetic acid, pH 5.5 with NH_3, 55°C. Left: actual sample including Dns-D-Leu as internal standard. Right: racemic mixture of Dns-D,L-Val.

Coverages of each bonded species, chelate (Γ_c) and diluent (Γ_d), were calculated from results of elemental and valine analysis. From the carbon percentage, C, obtained by elemental analysis, the number of moles of diluent per gram of material, n_d, was calculated by

$$n_d = \frac{\frac{C}{100} - 12 n_c I_c}{12\, I_d} \tag{2}$$

where n_c is the moles of chelate (valine) per gram bonded material and I_c and I_d are the number of carbon atoms per molecule of the chelate and diluent, respectively.

The silica content, W_s, of 1 g of bonded material is given by

$$W_s = 1 - (n_c M_c + n_d M_d) \tag{3}$$

where M_c and M_d are the molecular weights of the chelate and diluent, respectively. The coverages are then given by

$$\Gamma_i = n_i / W_s S_A \tag{4}$$

where S_A is the specific surface area of the silica gel.

Analysis of extent of removal of tert.-butyl ester protecting group. A sample of bonded silica gel, ≈ 150 mg, was placed in a 50-ml centrifuge tube. To this, 25 ml of TFA solution (95% or 100%) were added. The tube was closed with a septum and placed on a low-speed rotor. At various time intervals after centrifugation samples were directly injected into a GC column containing Porapak Q as the stationary phase. Another sample was removed for the analysis of the extent of stripping of the phase (see below). Isobutylene formation was quantitated by peak area, as compared to standards of similar concentrations.

Analysis of the extent of stripping of the phase. Samples of the mother-liquor were added to 75% TFA and treated as described above for hydrolysis and analysis of valine.

Mobile-phase composition

Due to the sensitive nature of ligand-exchange chromatography, care was used in the preparation of the mobile phases. Buffer solutions were prepared by delivering the correct weight of glacial acetic acid, and the pH was adjusted to 5.5 with concentrated ammonium hydroxide. Mobile phases were prepared by delivering the weight corresponding to 30 volume per cent acetonitrile to a volumetric flask. For mobile phases containing Cu^{2+}, the appropriate amount of 10 mM cupric acetate was added. The solutions were degassed under aspirator vacuum with rapid stirring for 5.0 min.

Determination of copper uptake

One chromatograph was outfitted with a six-port rotary valve, allowing for control of flow either through the column or bypassing the column directly to the

detector. The entire system was washed free of contaminants with methanol, water, 0.1 *M* EDTA in ≈10% acetonitrile, water and copper-free mobile phase. Switching the valve to "bypass", the entire chromatographic system, including the precolumn, but not the analytical column, was equilibrated with the copper-containing mobile phase. The valve was then switched back to begin a typical frontal chromatogram. Copper uptake, n (μmol), was calculated by the equation

$$n = (V_{50} - V_0)C_m \tag{5}$$

where V_{50} is the volume (ml) of mobile phase for the 50% breakthrough point, V_0 is the dead-volume (ml) of the column and C_m is the mobile-phase concentration (μmol/ml) of copper.

RESULTS AND DISCUSSION

An important aspect in the successful development of chemically bonded ligand-exchange phases is the selection of the chelate silane for bonding to the silica gel. In addition, the characterization of the synthesized bonded phase is similarly important in understanding details of the retention mechanism and thus in optimizing separations. Accordingly, the first part of this section will deal with the reasons for the selection of the specific silane for bonding, as well as the subsequent characterization of the bonded phase. After this examination, we shall turn to results obtained with various bonded phases.

Use of N-ω-(dimethylsiloxyl)undecanoyl-L-valine (IV) bonded phase

The selection of this chelate involved several factors, including availability of starting materials. As much as possible, we preferred to synthesize the total ligand prior to bonding to silica. In this manner, the product of each reaction step was isolated, and the species being bonded to the silica were completely known, including optical purity. An alternative approach involves first bonding a ligand that contains a reactive group, *e.g.*, amino, chloro, iodo, etc., followed by attaching the chelate moiety. While this approach can lead to successful separations, the distinct possibility exists of uncontrollable mixed phases resulting from an incomplete reaction. Such mixed phases could affect separation and retention; for example, residual amino groups would be available to participate in the ligand-exchange process.

Where possible, as noted in the Introduction, it is preferable to bond monofunctional silanes. A monofunctional silane ensures control over the spatial distance between neighboring chelates, which is essential when bonding mixed phases. Thus, polymerization prior to bonding for di- and trifunctional silanes could cause attachment of mixed phases with a non-uniform distribution. This would directly influence the column with respect to its retention characteristics as a diluted or concentrated phase. Moreover, there is ambiguity concerning the nature of the bonded surface when di- and trifunctional silanes are used[27].

The chiral amino acid has been linked to the silane via an amide bond, which is stable under all the chromatographic conditions. It may also be noted that the amide bond is advantageous since the bond can be hydrolyzed to release the amino acid for determination of the number of ligands bonded to the silica as well as the

optical purity of the bonded phase. This represents a convenient means of chemical characterization of the bonded phase.

Finally, the active site has been separated from the silica surface by a long alkyl leash. This spacer has been selected so that the chelate complex would be highly accessible to the solutes. The ligand-exchange kinetics, namely association/dissociation, may also be more rapid with a more flexible chelate. Moreover, the long hydrophobic chain may provide some protection of the silica surface from stripping by aqueous buffer salts.

Phase characterization

As already noted, the characterization of stationary phases by the determination of the chemical composition and coverage of bonded ligands on a silica surface is important. This characterization becomes all the more important for active stationary phases incorporating secondary chemical equilibria, especially when such phases involve the use of mixed bonded phases (diluted phases). In addition, the use of optically active phases for the separation of enantiomers requires a determination of the optical purity of the chiral ligands.

The characterization of bonded phases for LC has been dealt with by several techniques. The most popular method has been elemental analysis. While this approach can be useful, particularly in the case of alkyl-bonded phases, it is not a direct analysis. Moreover, it can be ambiguous for polar phases, while being insensitive to subtle differences involved in mixed phases.

A second approach involves titrating specific groups attached to the bonded phase. For example, with ion-exchange bonded phases, titration of the exchange groups can give some measure of the exchange capacity of that phase[28]. In the case of diol phases, periodate titration offers an estimate of the number of diol ligands[29].

More recently, direct methods of analysis have been developed. Generally, these methods involve stripping the bonded phase from the silica and then measuring the amount of ligand by techniques such as GC[30–33]. These approaches appear quite promising; however, care must be exercised with respect to the types of ligands that can be stripped intact and analyzed by a particular method.

We have selected a modified procedure of stripping of the ligand which appears to be convenient and allows direct measurement of the coverage and optical purity of the phase. Hydrolysis of the amide linkage between the alkyl spacer and the active site permits the direct measurement of the quantity and optical purity of the valine released from the silica gel.

Table I shows a comparison of bonded-phase coverages determined by elemental analysis and determined by analysis of the valine produced in the hydrolysis of the amide bond. For each phase, it can be seen that a good agreement exists between the coverages determined by the two methods. Hence, the approach of hydrolysis of the amide bond and subsequent analysis of the valine content via dansylation of the amino acid in HPLC is valid for the determination of bonded chelate coverage.

Table I further presents results of model studies obtained in the examination of conditions for binding chlorosilanes to silica. These studies were conducted with protected chelates using both methyl and *tert.*-butyl esters. The methyl esters were initially used as they are conventional and simple to synthesize. However, saponifi-

TABLE I

ANALYSIS OF BONDING COVERAGES OF CHELATE ESTERS ON SILICA

Room temperature reaction in pyridine.

Ester group	*Reaction time (h)*	*Coverage* (μmol/m²)*	*Coverage** (μmol/m²)*
Me	5	2.60	2.62
Me	10	2.61	2.56
Me	23	2.66	2.63
Me	48	2.68	2.68
tert.-Bu	5	2.62	2.61
n-Decyl***	10	2.98	–
n-Decyl	10	3.02§	–

* Elemental analysis.
** Direct analysis of valine for hydrolysis with 75% TFA.
*** *n*-Decyldimethylchlorosilane.
§ Reflux in pyridine.

cation of methyl esters is typically conducted under basic conditions, which are not feasible in this study, as these conditions would affect the stability of the silica itself. Hydrolysis under various acid conditions was found to be non-specific for the methyl ester group. Hence, for bonded-phase synthesis, it was necessary to use the *tert.*-butyl group, for which milder deblocking conditions were possible. As can be seen from Table I, both the methyl and the *tert.*-butyl esters gave comparable coverage.

It is further observed in Table I that the *n*-decyl phase yielded roughly 3 μmol/m² after chemical bonding for 10 h in pyridine at either room temperature or reflux. Also, the protected chelate yielded the same coverage, ≈2.6 μmol/m², under either condition. Hence, for convenience and minimization of potential side reactions, it was decided to bond in pyridine at room temperature. Table I also reveals that coverages were roughly constant after 5 h of bonding. Subsequent phases were bonded, therefore, for at least 5 h.

TABLE II

VALINE ANALYSIS OF CHELATE BONDED PHASE

Hydrolysis with 75% TFA, reflux. Elemental analysis: 2.61 μmol/m².

Reaction time	*Amount (μmol/m²) ± 0.6%**	*% Optical purity ± 0.4%**
5 min	0.24	98.9
10 min	0.43	98.0
1 h	1.35	95.8
2 h	1.97	93.5
5 h	2.54	90.6
20 h	2.57	89.3

* Based on determination of released L-valine.

TABLE III

RACEMIZATION OF COMPOUND I DURING HYDROLYSIS

Conditions: 75% TFA, reflux. Optical purity of L-valine >99.8% after 30 h under these conditions.

Reaction time	*% Optical purity ± 0.4%*
5 min	99.6
10 min	99.1
20 min	97.9
1 h	94.6
5 h	90.8
16 h	89.7

Returning to the hydrolysis of the amide bond, the conventional conditions for this reaction, *e.g.*, 6 *M* HCl, reflux, were found to yield irreproducible results, probably due to the poor wettability of the bonded phases. The hydrolysis was thus performed by using 75% TFA with D-leucine as an internal standard. Table II shows that after 5 h of hydrolysis, the measured coverage is within 2.5% of that determined by elemental analysis (2.61 μmol/m^2). As shown in Fig. 2, injection of the mixture provided for the potential appearance of three peaks: dansyl derivatives of D-leucine, D-valine and L-valine. The total valine content was obtained through a summation of the peak areas of the D- and the L-valine.

Table III shows the optical purity of the released valine during the hydrolysis of I, *i.e.*, of the amide *tert.*-butyl ester in solution. The optical purity of the released valine decreased in the early stages of the reaction and leveled off, whereas that of free L-valine remained unchanged. Under these conditions, the *tert.*-butyl ester I was rapidly decomposed, yielding the N-acyl derivative of the amino acid, which was gradually hydrolysed to produce valine. Racemization apparently occurred during the intermediate stage.

Table II shows the apparent coverage and optical purity of the bonded phase. Clearly, in order to determine the true optical purity of the bonded chelate, an extra-

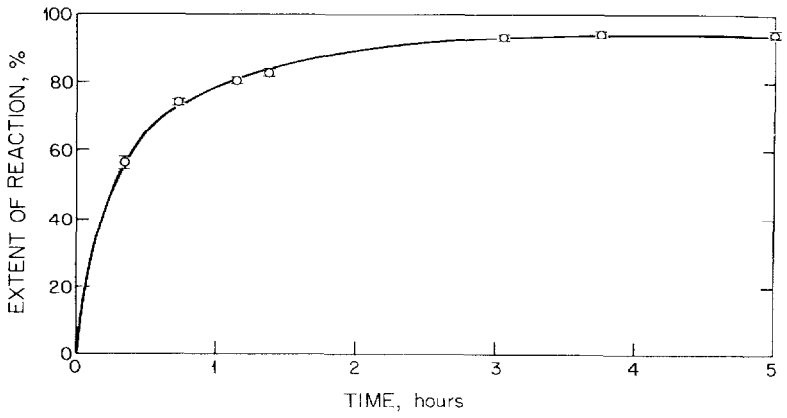

Fig. 3. Rate of removal of *tert.*-butyl ester protective group; hydrolysis in 95% TFA, room temperature.

polation to zero time of hydrolysis is necessary. For practical purposes, optical purity was determined for concentrated phases by sampling the reaction after 10 min. In the case of the diluted phases, interfering peaks, due to the low amount of valine, prohibited the analysis after such a short time and, therefore, a reaction for 30 min was employed. Separate studies revealed that the rate of racemization was comparable to that of the concentrated phase. As analyzed, the phases in this paper have optical purities $\geqslant 99\%$.

The final step in the bonding procedure was the removal of the *tert.*-butyl ester group to form the bonded chelate. The by-product of the hydrolysis of a *tert.*-butyl ester is isobutylene, which was quantitatively analyzed by GC. Fig. 3 shows the extent of isobutylene formation by the sample of a bonded phase, with 95% TFA at room temperature. Unfortunately, the reaction was accompanied by the undesirable side reaction of stripping of the entire ligand from the surface. Fig. 4 shows the extent of stripping of the bonded ligand under these conditions; after 2 h, 19% was found to be removed. That this stripping was not due to hydrolysis of the amide bond could be verified by the fact that no free valine was found in the reaction mixture. Fig. 4 also shows that the extent of stripping with neat TFA was greatly reduced, while isobutylene evolution was completed after $\leqslant 2$ h. It is also noted that 7% of the phase was stripped rapidly while the remainder appeared much more slowly. This is suggestive of the fact that a small portion of the phase is more vulnerable to hydrolysis.

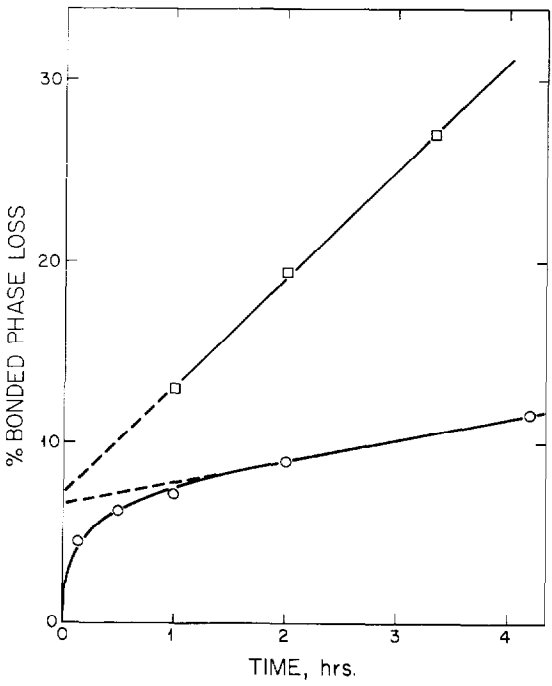

Fig. 4. Extent of bonded phase stripping, as a function of hydrolysis conditions and time, □, 95% TFA; ○, neat TFA, room temperature.

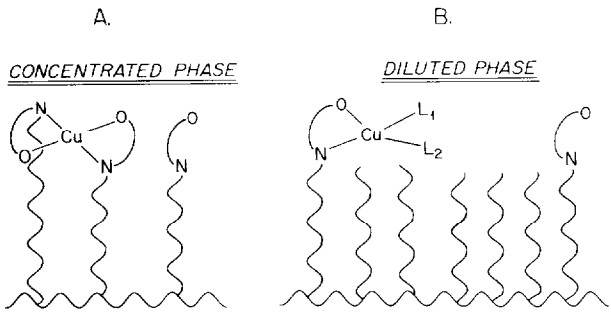

Fig. 5. Schematic of possible bis complex [2:1 chelate:Cu(II)] on concentrated bonded phase and mono complex [1:1 chelate:Cu(II)] on diluted phase.

Diluted vs. concentrated phase

As already noted, for those phases in which the coverage of active chelate ligand is relatively high, the formation of complexes, $\geqslant$, 2:1 chelate:copper (see Fig. 5A), is likely. At present it is unclear as to the exact complexes that form on the concentrated phase, however, for purposes of clarity, we shall refer to these complexes as bis. Such bis complexes could be formed simultaneously with mono complexes, *i.e.*, 1:1 chelate:copper. In order to provide a simpler and more controllable bonded-phase system, we have designed diluted phases in which, assuming even random bonding, the formation of the bis complex is of low probability. In such a case, as shown in Fig. 5B, exchange processes could only occur between ligands from the mobile phase.

Fig. 6 illustrates the design of a diluted phase, with *n*-decyl as diluent. It is observed that, in the fully extended conformation, the distance between the silicon atom and the amido carbonyl is $\approx$14 Å. Therefore, a distance of $\geqslant$28 Å between neighboring chelates is sufficient to preclude the formation of a bis copper–chelate

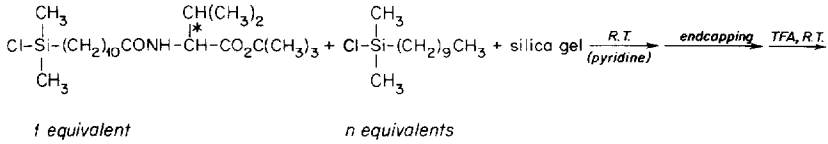

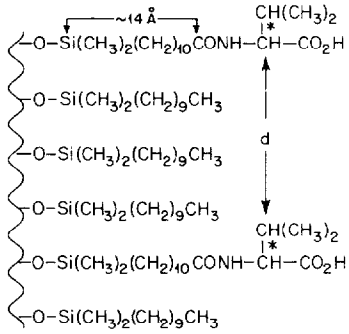

Fig. 6. Strategy for bonding of C_{10} diluted phase for mono chelate–Cu(II) complexation.

TABLE IV

CHARACTERISTICS OF VARIOUS BONDED PHASES

Phase	*Diluent*	*Chelate coverage (μmol/m^2)*	*Total coverage (μmol/m^2)*
C_4	$-Si(CH_3)_2(CH_2)_3CH_3$	0.15	3.1
C_{10}	$-Si(CH_3)_2(CH_2)_9CH_3$	0.13	3.1
C_{20}	$-Si(CH_3)_2(CH_2)_{19}CH_3$	0.09	3.1
Ether	$-Si(CH_3)_2(CH_2)_3(OCH_2CH_2)OCH_3$	0.14	2.4
Conc.	None	2.4	2.4
Decyl	$-Si(CH_3)_2(CH_2)_9CH_3$	None	2.5

complex. In the limiting case of closest packing, this spacing is approximated by chelate coverages of $\leqslant 0.24$ μmol/m^2, assuming an idealized flat surface. It is to be noted that in this case higher coverages without a significant formation of a bis complex are probable, as the free energy gained in forming such a complex must overcome steric and conformational restrictions. This thermodynamic balance allows for mono complexation even in the case of smaller interchelate distances. Thus, even though at 0.24 μmol/m^2 the spacing may have a random distribution, the assumption of predominantly mono complexation is reasonable. The concentrated phase, on the other hand, has a mean distance of ≈ 10 Å between neighboring chelates. This is expected to enhance greatly the likelihood of a bis complex.

TABLE V

COMPARISON OF CONCENTRATED AND DILUTED PHASES FOR THE RETENTION AND SEPARATION OF Dns-D,L-AMINO ACIDS

10^{-4} *M* Cu(II), 30% acetonitrile, 0.035 *M* acetic acid, pH 5.5 with NH_3, 55°C.

Dns-AA		*Conc.**		C_{10}**	
		k'	α	k'	α
Ala	D	1.57	no sepn.	4.90	2.34
	L			11.45	
Val	D	1.80	no sepn.	4.32	2.75
	L			11.88	
Leu	D	3.31	no sepn.	7.25	3.44
	L			24.95	
Ser	D	1.46	1.15	3.69	2.17
	L	1.68		8.00	
Thr	D	1.29	1.16	3.01	3.38
	L	1.49		10.20	
Asn	D	1.30	1.44	4.69	3.33
	L	1.87		15.64	
Asp	D	1.61	1.60	1.65	2.70
	L	2.58		4.46	
Glu	D	0.79	1.19	1.05	1.47
	L	0.94		1.54	

* 140 μmol Cu(II) loaded.

** 3.6 μmol Cu(II) loaded.

We synthesized a series of phases with different diluents, as detailed in Table IV. Included in this table, as well, are the coverages of the concentrated phase and a reference decyl phase containing no chelate. Each phase with chelate was found to be optically pure at a level $\geqslant 99\%$. All of the diluted phases have chelate coverages below 0.24 μmol/m^2, allowing mainly mono complex formation, even though the porous silica matrix is not an idealized flat surface. Each diluent has been chosen to probe the influence of the environment around the active site with respect to retention and separation (see below).

Consider, first, the comparison of the concentrated phase with a diluted phase, in particular the C_{10} diluted phase. After some preliminary experiments, we set as common mobile phase conditions for this comparison: 10^{-4} *M* Cu(II), 30% acetonitrile, 0.035 *M* acetic acid, pH 5.5 with NH_3, 55°C.

A series of eight representative Dns-AAs were chromatographed on both columns, and Table V presents the results of this study. We first note that under these mobile phase conditions, 140 μmol of Cu(II) were loaded onto the concentrated phase, whereas only 3.6 μmol of Cu(II) were loaded on the diluted phase —a difference of roughly 40-fold. In spite of this large difference, retention was found to be smaller (as much as 10-fold) on the concentrated phase *versus* the diluted phase. Moreover, on the concentrated phase, separation was not observed for the hydrophobic Dns-AAs and only for the polar tridentate solutes was enantioselectivity observed. On the other hand, for the diluted phase, high α values were observed for all

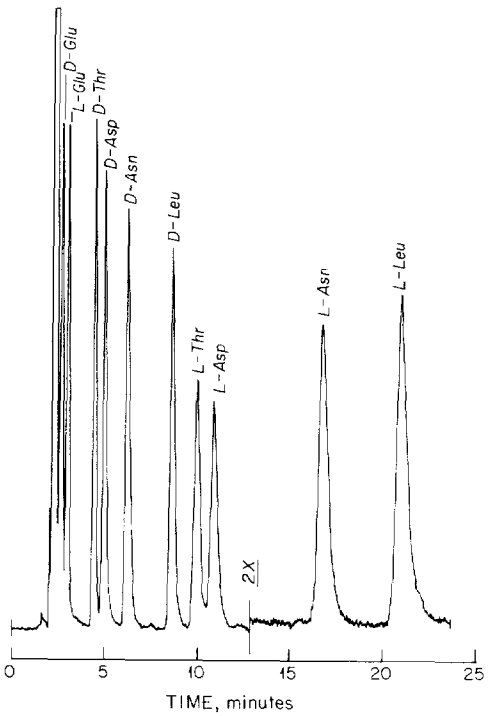

Fig. 7. Separation of Dns-D,L-amino acids on C_{10} diluted phase, 10^{-4} *M* Cu(II), 30% acetonitrile, 0.035 *M* acetic acid, pH 5.5 with NH_3, 55°C. 2× Indicates a change in the attenuation.

the solutes. Hence, under these mobile phase conditions, the two bonded phases are very different from one another, and the retention and separation possibilities on the diluted phase are clearly evident. Fig. 7 shows a typical chromatogram of a series of Dns-AAs on the C_{10} diluted phase. Good column performance and relatively good peak symmetry are observed in this separation.

Large loading of Cu(II) on the concentrated phase is expected, given the 20-fold higher surface concentration of bonded chelates. However, it is necessary to examine in more detail the retention process, in order to understand the much larger retention on the diluted phase. It is important to demonstrate, first, that the effects observed in Table V were a consequence of the ligand-exchange process and not due to other retention behavior differences. We thus examined the influence of Cu(II) on retention of the Dns-AAs with no bonded chelate groups present, by studying the decyl bonded-phase column. The coverage of this phase, after identical treatment as the chelate-containing phases, was 2.5 μmol/m^2 (see Table IV).

Table VI presents results for the retention of Dns-AAs on the decyl column under the same mobile phase conditions with and without Cu(II). We first note that only 0.16 μmol of Cu(II) were loaded on this column at a mobile phase concentration of 10^{-4} M, a value which is only 4% of that loaded on the C_{10} diluted phase. Thus, by analogy, under these conditions, uptake of Cu(II) on chelate-containing phases by species other than the chelate is small. From these results, we can conclude that the Cu(II) loaded onto the diluted phase represents the quantity of activated chelate available for ligand-exchange chromatography. We further note that the presence of 10^{-4} M Cu(II) in the mobile phase does not affect the retention of the solutes. Hence, other interactions in either the mobile or stationary phase not involving the active site do not influence, significantly, retention under the mobile phase conditions of Table V.

The next question was whether the diluent itself was a cause of the increased retention on the diluted phase. This question could be answered by examining retention of the Dns-AAs on the diluted phase without copper present in the mobile phase.

TABLE VI

EFFECT OF Cu(II) ON RETENTION (k')

Decyl phase, treated in similar manner to the chelate phases. 30% Acetonitrile, 0.035 M acetic acid, pH 5.5 with NH_3, 55°C.

Dns-AA	*[Cu(II)] (M)*	
	0	*10^{-4}**
Ala	1.04	1.10
Val	1.84	1.79
Leu	2.71	2.80
Phe	3.09	3.13
Ser	0.68	0.70
Thr	0.84	0.84
Asn	0.50	0.50
Asp	0.40	0.37
Glu	0.39	0.39

* 0.16 μmol Cu(II) loaded.

TABLE VII

COMPARISON OF DILUTED PHASE

10^{-4} *M* Cu(II), 30% acetonitrile, 0.035 *M* acetic acid, pH 5.5 with NH_3, 55°C.

Dns-AA	*Ether 10.2**		C_4 *6.1*		C_{10} *3.6*		C_{20} *3.9*	
	k'	α	k'	α	k'	α	k'	α
D-Ala	5.62	2.51	5.33	2.58	4.90 (0.51)**	2.34	11.86 (0.61)**	2.93
L-Ala	14.12		13.72		11.45		34.76	
D-Val	3.44	2.84	3.96	2.80	4.32 (0.94)	2.75	10.80 (1.29)	3.3
L-Val	9.78		11.06		11.88		35.6	
D-Leu	4.49	4.08	6.10	3.85	7.25 (1.50)	3.44	–	–
L-Leu	18.30		23.51		24.95			
D-Ser	4.87	2.65	4.32	2.74	3.69 (0.34)	2.17	8.72 (0.31)	2.57
L-Ser	12.89		11.84		8.00		22.43	
D-Thr	3.23	4.07	3.03	4.16	3.01 (0.41)	3.38	6.92 (0.45)	4.00
L-Thr	13.14		12.63		10.20		27.66	
D-Asn	6.22	4.45	5.29	4.81	4.69 (0.29)	3.33	10.50 (0.21)	3.98
L-Asn	27.70		25.44		15.64		41.75	
D-Asp	3.61	3.52	2.54	3.66	1.65 (0.16)	2.70	6.62 (0.05)	4.43
L-Asp	12.69		9.30		4.46		29.35	
D-Glu	2.10	1.62	1.52	1.72	1.05 (0.18)	1.47	2.57 (0.06)	1.71
L-Glu	3.39		2.61		1.54		4.39	

* Cu(II) loaded (μmol).

** k' values with no Cu(II) present in mobile phase.

It was found that retention on the C_{10} phase without copper present was, in general, less than 10% of that with copper present at 10^{-4} *M*, particularly in the case of the L-forms (see values in parentheses in Table VII). That copper-free chelates do not contribute to retention is verified by the behavior on the concentrated phase. On this phase, there was no retention with copper absent from the mobile phase. It is thus clear that the causes of increased retention on the diluted phase relative to that on the concentrated phase are predominantly related to the ligand-exchange process itself.

It should be noted that at this time the actual structures of the mono and bis chelate:copper complexes on the surface are not known. In pure aqueous solution bidentate Cu(II) complexes with, *e.g.*, N-acetylglycine have not been demonstrated[34]. The mechanism of chiral recognition and structures of the surface chelate:copper complexes in the mixed aqueous–organic media require further study.

Retention models

Diluted phase. It is possible to develop a simple model of retention, for an ideal diluted phase, as shown below.

We may first consider complexation of a Dns-AA with the activated chelate, *i.e.*, chelate containing copper

$$S_m + (Cu\text{–}Ch)_s \overset{K_c}{\rightleftharpoons} (S\text{–}Cu\text{–}Ch)_s \qquad (6)$$

where S is the Dns-AA, Cu the copper, Ch the chelate and the subscripts m and s the mobile and stationary phases, respectively. In this simple equation, we have not considered complexation of the Dns-AA with copper in the mobile phase nor the other possible ligands involved in the exchange process. The complexation reaction of eqn. 6 can be assigned the equilibrium constant K_c. For chiral recognition to occur, the K_c values must be different for the D- and L-amino acids.

A second contribution to retention can involve the distribution of solute between the mobile and stationary phases:

$$S_m \overset{K_0}{\rightleftharpoons} S_s \tag{7}$$

This distribution process is given a constant value K_0 which is assumed to be identical for both D- and L-isomers.

Using this simple equilibrium model, we can relate the capacity factor of any Dns-AA to the complexation and distribution constants through eqn. 8

$$k' = \varphi\,(K_0 + K_c\,[\text{Cu–Ch}]_s) \tag{8}$$

where φ is the phase ratio. Eqn. 8 can be simplified to eqn. 9

$$k' = \varphi\,(K_0 + K_c\,[\text{Cu}]_s) \tag{9}$$

if the copper loaded on the stationary phase is bound only by the chelate and in a 1:1 ratio. Eqn. 9 can be rearranged to:

$$k'^* = \frac{k' - \varphi K_0}{[\text{Cu}]_s} = \varphi K_c \tag{10}$$

Thus, by normalizing to the amount of copper loaded on such a stationary phase, a parameter k'^* is obtained, which is proportional to K_c. Note also, that by measuring k' without Cu(II) present in the mobile phase, φK_0 can be estimated and subtracted from k' found with Cu(II) present. (The amount of copper loaded on the stationary phase is small in relation to the total bonded phase.)

The α value for a D/L pair of a Dns-AA can be written from eqn. 9 as

$$\alpha = \frac{k'_L}{k'_D} = \frac{K_0 + K_c^L\,[\text{Cu}]_s}{K_0 + K_c^D\,[\text{Cu}]_s} \tag{11}$$

and from eqn. 10:

$$\alpha^* = \frac{k'^*_L}{k'^*_D} = \frac{k'_L - \varphi K_0}{k'_D - \varphi K_0} = \frac{K_c^L}{K_c^D} \tag{12}$$

From the above analysis, it is seen that a straightforward retention model on the

idealized diluted phase can be developed by virtue of the isolation of the active site from other complexing groups on the stationary phase. We next consider retention on the concentrated phase in order to interpret the major trends of Table V.

Concentrated phase. As already noted, on the concentrated phase the bis complex is assumed to be the predominant species due to the close proximity of the bonded chelates. Further assuming that bidentate Dns-AA complexation with Cu(II) occurs only through the mono Cu(II)–chelate complex, an analysis similar to that used in the examination of complexation in GC[35] and LEC of amino acids[20] can be developed.

Formation of the bis complex from the mono complex in the stationary phase can be written as

$$(\text{Cu–Ch})_s + (\text{Ch})_s \overset{K_2}{\rightleftharpoons} (\text{Ch–Cu–Ch})_s \tag{13}$$

where again we have omitted other mobile phase ligands that fill the coordination sphere of the metal complex. The concentration of the mono complex, $(\text{Cu–Ch})_s$ is then:

$$[\text{Cu–Ch}]_s = K_2^{-1} \cdot \frac{[\text{Ch–Cu–Ch}]_s}{[\text{Ch}]_s} \tag{14}$$

Substitution of eqn. 14 into eqn. 8 yields:

$$k' = \varphi \left(K_0 + K_c K_2^{-1} \cdot \frac{[\text{Ch–Cu–Ch}]_s}{[\text{Ch}]_s} \right) \tag{15}$$

When the bis complex is the predominant form

$$[\text{Cu}]_s \approx [\text{Ch–Cu–Ch}]_s \tag{16}$$

and

$$[\text{Ch}]_s \approx [\text{Ch}]^0 - 2[\text{Cu}]_s \tag{17}$$

where $[\text{Ch}]^0$ is the total bonded chelate concentration. Substitution of eqns. 16 and 17 into 15 yields:

$$k' = \varphi \left(K_0 + K_c K_2^{-1} \cdot \frac{[\text{Cu}]_s}{[\text{Ch}]^0 - 2[\text{Cu}]_s} \right) \tag{18}$$

Eqns. 9 and 18 can now be used to explain Table V.

It can be assumed that the complexation term in eqn. 9 will be larger than that in eqn. 18 for two reasons. First, K_2^{-1} is expected to be much less than unity due to

the gain in free energy in forming the bis complex. Secondly, under the conditions of Table V, it was found that $[Ch]^o/[Cu]_s \approx 4$. Thus, $K_2^{-1}/2$ is the "effective" $[Cu]_s$ available for complexation on the concentrated phase. In other words, the factor of 40 in the copper loading of the concentrated phase is overcome by virtue of the bis complex.

We have already noted that the K_0 value in the C_{10} phase can be estimated from the retention of the solute without copper present in the mobile phase. On the other hand, in the case of the concentrated phase, K_0 can no longer be determined from retention on the column without copper present. The large amount of loaded copper may significantly alter the polar characteristics of the stationary phase. Thus, polar–polar interactions, perhaps even involving monodentate copper–solute interactions, may contribute to K_0.

Retention on the concentrated phase is lower than on the diluted phase as a consequence of the reduction in Dns-AA complexation with copper due to the formation of the bis Cu(II)–chelate complex. Moreover, since the complexation term contains the chiral recognition, it is understandable that the relative contribution of K_0 to the overall retention is greater in the case of the concentrated phase, and the separation of Dns-D,L-AAs would be lower on this phase.

This analysis has shown that the diluted phase provides a simpler phase system for the interpretation and control of LEC. Accordingly, we have not continued the examination of the concentrated phase and instead focused our efforts on the diluted phase.

Role of diluent type

With respect to diluted phases, an important question is the role of the type of diluent on retention and separation. Since the active site is isolated from other sites, it should be possible to manipulate the environment around the complex by varying the chemical structure of the diluent.

We have thus synthesized four different diluted phases, as detailed in Table IV and shown diagrammatically in Fig. 8. Three of these phases are *n*-alkyl diluted phases; a C_4 phase, in which the diluent is shorter than the chelate spacer, a C_{10}

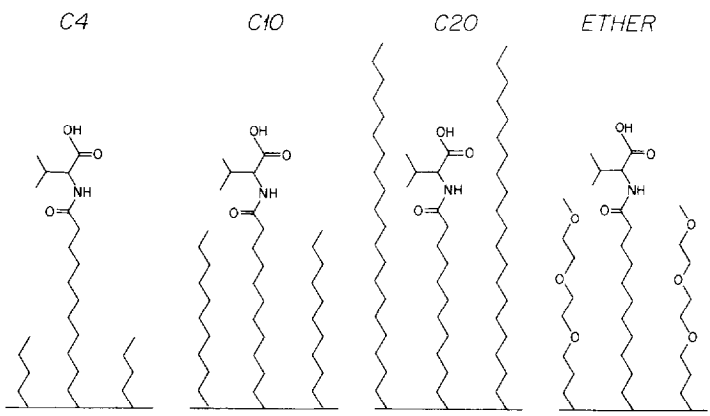

Fig. 8. Schematic illustration of various diluted phases.

phase, in which the diluent is roughly of the same length as the spacer and a C_{20} phase, in which the diluent is much longer than the spacer. A fourth phase consisted of a hydrophilic diluent, namely a polyether, of roughly the same length as the spacer of the chelate itself. Thus, both hydrophilic and hydrophobic environments could be adjusted around the chelate complex. Of course, it is not necessary that the phases be aligned and fully extended, as shown in Fig. 8; however, the figure does emphasize the potentially different environments possible. As shown in Table IV, a sufficiently small surface concentration of chelate was formed on each column to yield only the mono chelate–copper complex.

We selected eight representative Dns-AAs for examination of the diluted phases. Using the same conditions, retention and separation was measured on the four diluted phases, and the results are presented in Table VII. It can be seen that the retention does not vary in a regular fashion, although the k' values on the C_{20} phase do appear somewhat higher than on the other phases. Also, the differences in α values between the columns are not great. However, relatively high α values are found in certain cases, *e.g.*, Dns-D,L-Asn on the C_4 phase, $\alpha = 4.81$. An interesting point, however, is that the amount of copper loaded on each column varies significantly. The highest value, roughly 10 μmol, occurs on the ether phase, whereas the C_{10} and C_{20} diluted phases contain about one third as much copper. The amount of copper loaded on each diluted phase is a consequence, in part, of the hydrophilic/hydrophobic environment in the vicinity of the chelate.

In order to obtain insight into the influence of the diluent on retention and selectivity, we have used the normalizing parameter k'^*, defined in eqn. 10 assuming an idealized diluted phase. In this model, the value of k'^* is proportional to K_c, if φK_0 can be neglected. It is important to note, that in this normalization we assume as an approximation that $[Cu]_s$, the measured copper uptake, is a result of 1:1 chelate:copper complex formation, neglecting any contribution of higher ratio chelate: copper species. Separate studies revealed that the Dns-AAs were unretained on the ether and C_4 diluted phases when no Cu(II) was present in the mobile phase. Thus, for these columns the φK_0 value of eqn. 8 can be assumed to be negligible. For the C_{10} and C_{20} phases, retention without Cu(II) in the mobile phase was observed to be small but finite (see Table VII). As discussed previously, it is possible to correct the k' values by subtracting the retention without Cu(II) present, to obtain k'^* values proportion to K_c; however, for the analysis in this paper we have neglected this small correction.

Fig. 9 shows a plot of k'^* values for four Dns-L-AAs *versus* diluent type. In all cases, for the compounds shown and the others studied, there was a regular increase of k'^* from the ether to the C_{20} phase. More interestingly, these corrected values reveal selectivity differences between amino acids. The retention differences between the ether and the C_{20} columns were small in the case of hydrophilic Dns-AAs, such as glutamic acid, whereas for the hydrophobic amino acids the differences were large. Also, retention changes are observed between the C_4 and the C_{10} phases. The results of Fig. 10 indicate that the diluent can play a significant role with respect to selectivity when active chemical equilibria are involved. Indeed, we shall show in the next section an example where this additional selectivity plays an important role on separation. It can be concluded that the chemical nature of the diluent influences the environment of the chelate–Cu–solute complex.

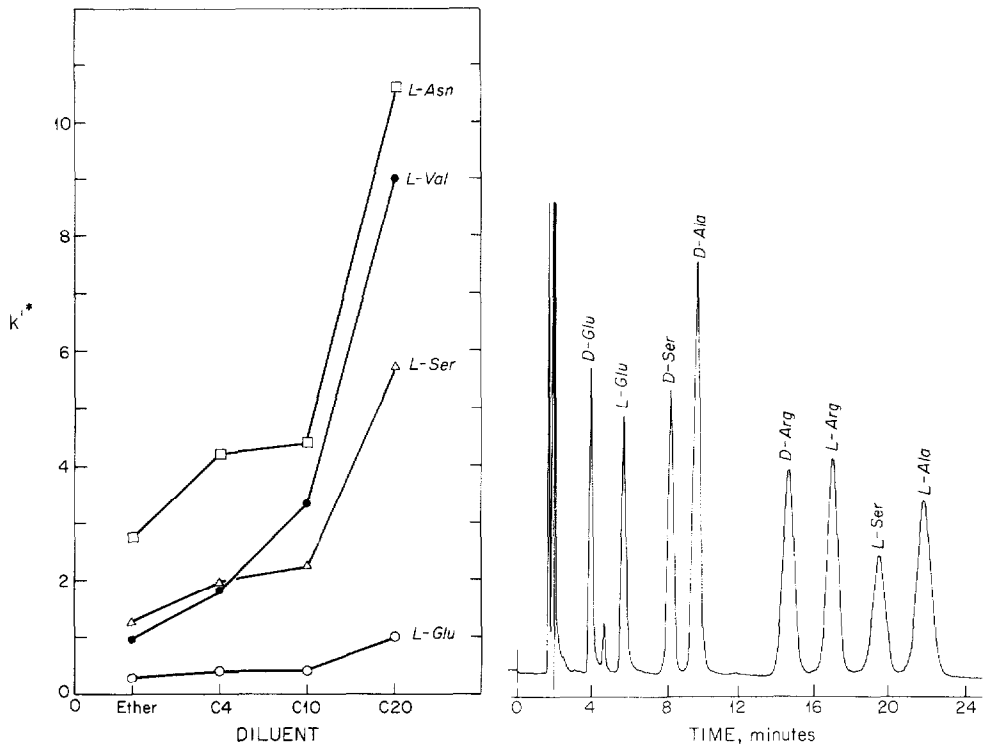

Fig. 9. Capacity factors, normalized for Cu(II) loading of Dns-L-amino acids, on various diluted phases. Mobile phase conditions: see Fig. 8.

Fig. 10. Separation of Dns-D,L-amino acids on C_4 diluted phase. Mobile phase conditions: see Fig. 8.

Returning to Table VII, it is observed that the relative retentions of the D,L-isomers do not vary significantly as a function of the diluent, with the possible exception of slightly higher α values on the C_{20} diluted phase. This result may mean that the factors involved in chiral recognition are not the same as those involved in the solvation of the complex. Thus, for these solutes the type of diluent does not appear to play a significant role with respect to chiral recognition. However, as we have already noted, the selectivity between different amino acids is a function of the diluent.

Applications

We have found the diluted phases, relative to concentrated phases, but also to yield high separation factors for chiral species. Moreover, performances with regard to efficiency and peak symmetry similar to those obtained with chiral additives[3] have been achieved. Fig. 10 shows a chromatogram on the C_4 diluted phase with approximately 4000 theoretical plates and peak symmetry factors of 1.0 in all cases except Dns-Glu where the peak symmetry is approximately 1.4. This result demonstrates that high-performance LEC with chemically bonded phases can be achieved.

As an example of the selectivity possible with different diluents, Fig. 11 shows

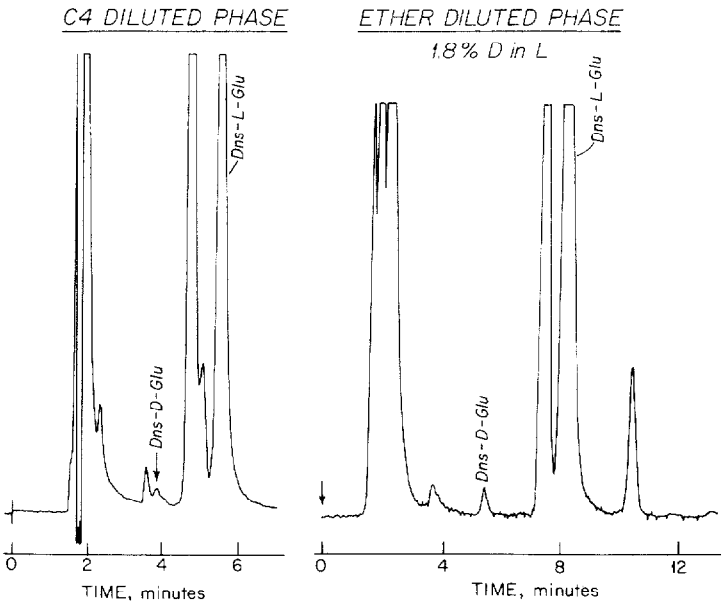

Fig. 11. Analysis of Dns-D,L-glutamic acid on two diluted phases. Mobile phase conditons: see Fig. 8.

the chromatography of a hydrolyzed drug, containing a moiety of L-glutamic acid. After hydrolysis, the material is dansylated and separated as shown. On the left side of Fig. 11, a chromatogram is presented in which the Dns-D-Glu is eluted in a region containing other components. It would be difficult to quantitate this peak from this chromatogram. While better mobile phase conditions may be found, a second option is to use a different diluted phase, namely the ether diluted phase, as shown on the right side of Fig. 11. Here, the Dns-D-Glu elutes in an interference-free region. The selectivity differences between the two diluted phases is clearly shown.

CONCLUSIONS

Bonded ligands, by virtue of their fixed attachment to the silica surface, provide unusual possibilities for chemical manipulation of selectivity. This paper has shown that by effectively creating an "infinite" dilution environment at "finite concentration"[36], a simplified, controllable phase system can be developed. Previous work, on LEC of amino acids, showed non-linearity of retention and enantioselectivity due to formation of different ratios of mono/bis complexes when "concentrated" bonded chelate phases were used[20]. Diluted phases thus offer potential advantages over concentrated phases when specific solute–bonded ligand interactions take place. Mixed bonded phases are also being studied as an alternative approach to ion-pair chromatography[37].

By virtue of the homogeneity of the environment surrounding the active ligand-exchange site, it has been possible to develop a simple model for understanding and controlling retention and separation. Moreover, the diluted phases have been shown to yield high-performance separations with high enantioselectivity. Finally,

we have illustrated that the environment around the active site can be manipulated by the judicious selection of the diluent.

A second paper will deal with further details of diluted phases for ligand-exchange chromatography. This paper will also consider mechanistic details of the ligand-exchange process. The role of buffer concentration, organic modifier and temperature on retention and separation will be explored.

ACKNOWLEDGEMENTS

The authors gratefully acknowledge the National Science Foundation for support of this research. Contribution No. 168 from the Institute of Chemical Analysis.

REFERENCES

1 V. Davankov, *Advan. Chromatogr.*, 18 (1980) 139.
2 W. F. Lindner, in R. W. Frei and J. F. Lawrence (Editors), *Chemical Derivatization in Analytical Chemistry*, Vol. 2, Plenum, New York, 1982, p. 145.
3 J. N. LePage, W. Lindner, G. Davies, D. E. Seitz and B. L. Karger, *Anal. Chem.*, 51 (1979) 433.
4 P. E. Hare and E. Gil-Av, *Science*, 204 (1979) 1226.
5 W. Lindner, J. N. LePage, G. Davies, D. E. Seitz and B. L. Karger, *J. Chromatogr.*, 185 (1979) 323.
6 V. A. Davankov, A. S. Bochkov, A. A. Kurganov, P. Roumeliotis and K. K. Unger, *Chromatographia*, 13 (1980) 677.
7 E. Gil-Av, A. Tishbee and P. E. Hare, *J. Amer. Chem. Soc.*, 102 (1980) 5115.
8 Y. Tapuhi, N. Miller and B. L. Karger, *J. Chromatogr.*, 205 (1981) 325.
9 C. Gilon, R. Leshem and E. Grushka, *J. Chromatogr.*, 203 (1981) 365.
10 V. A. Davankov, A. S. Bochkov and Yu. P. Belov, *J. Chromatogr.*, 218 (1981) 547.
11 S. Weinstein, M. H. Engel and P. E. Hare, *Anal. Biochem.*, 121 (1982) 370.
12 V. A. Davankov, S. V. Rogozhin, A. V. Semechkin and T. P. Sachkova, *J. Chromatogr.*, 82 (1973) 359.
13 V. A. Davankov, S. V. Rogozhin and A. V. Semechkin, *J. Chromatogr.*, 91 (1974) 493.
14 B. Lefebvre, R. Audebert and C. Quivoron, *J. Liquid Chromatogr.*, 1 (1978) 761.
15 V. A. Davankov and A. A. Kurganov, *Chromatographia*, 13 (1980) 339.
16 H. Engelhardt and S. Kromidas, *Naturwissenschaften*, 67 (1980) 353.
17 W. Lindner, *Naturwissenschaften*, 67 (1980) 354.
18 K. Sugden, C. Hunter and G. Lloyd-Jones, *J. Chromatogr.*, 192 (1982) 228.
19 G. Gübitz, W. Jellenz and W. Santi, *J. Chromatogr.*, 203 (1981) 377.
20 J. Boué, R. Audebert and C. Quivoron, *J. Chromatogr.*, 204 (1981) 185.
21 P. Roumeliotis, K. K. Unger, A. A. Kurganov and V. A. Davankov, *J. Chromatogr.*, 255 (1983) 51.
22 P. Cuatrecasas, M. Wilchek and C. B. Anfinsen, *Proc. Nat. Acad. Sci. U.S.*, 61 (1968) 636.
23 R. Roeske, *J. Org. Chem.*, 28 (1963) 1251.
24 G. W. Anderson, J. E. Zimmerman and F. M. Callahan, *J. Amer. Chem. Soc.*, 89 (1967) 5012.
25 J. L. Speier, J. A. Webster and G. H. Barnes, *J. Amer. Chem. Soc.*, 79 (1957) 974.
26 Y. Tapuhi, D. E. Schmidt, W. Lindner and B. L. Karger, *Anal. Biochem.*, 115 (1981) 123.
27 N. Becker and K. Unger, *Z. Anal. Chem.*, 304 (1980) 374.
28 M. Gimpel and K. K. Unger, *Chromatographia*, 16 (1982) 117.
29 F. E. Regnier and R. Noel, *J. Chromatogr. Sci.*, 14 (1976) 316.
30 M. Verzele, P. Mussche and P. Sandra, *J. Chromatogr.*, 190 (1980) 331.
31 H. Hemetsberger, H. Klar and H. Ricken, *Chromatographia*, 13 (1980) 277.
32 J. Erard and E. Kovats, *Anal. Chem.*, 54 (1982) 193.
33 H.-G. Genieser, D. Gabel and B. Jastorff, *J. Chromatogr.*, 244 (1982) 368.
34 D. L. Rabenstein, *Can. J. Chem.*, 50 (1972) 1036.
35 B. Feibush, M. F. Richardson, R. E. Sievers and C. S. Springer, Jr., *J. Amer. Chem. Soc.*, 94 (1972) 6717.
36 M. A. Kraus and A. Patchornik, *Isr. J. Chem.*, 17 (1978) 298.
37 J. B. Crowther and R. A. Hartwick, *Chromatographia*, 16 (1982) 349.